LBL-23058 c. 2
Preprint

Lawrence Berkeley Laboratory
UNIVERSITY OF CALIFORNIA

Materials & Chemical Sciences Division

RECEIVED
LAWRENCE
BERKELEY LABORATORY

MAY 23 1988

LIBRARY AND
DOCUMENTS SECTION

Submitted to Surface Science

The Preparation and Characterization of Rhenium Modified Pt(111) and Pt(100), and Platinum Modified Re(0001) Single Crystal Surfaces

D.J. Godbey and G.A. Somorjai

November 1987

TWO-WEEK LOAN COPY
This is a Library Circulating Copy
which may be borrowed for two weeks.

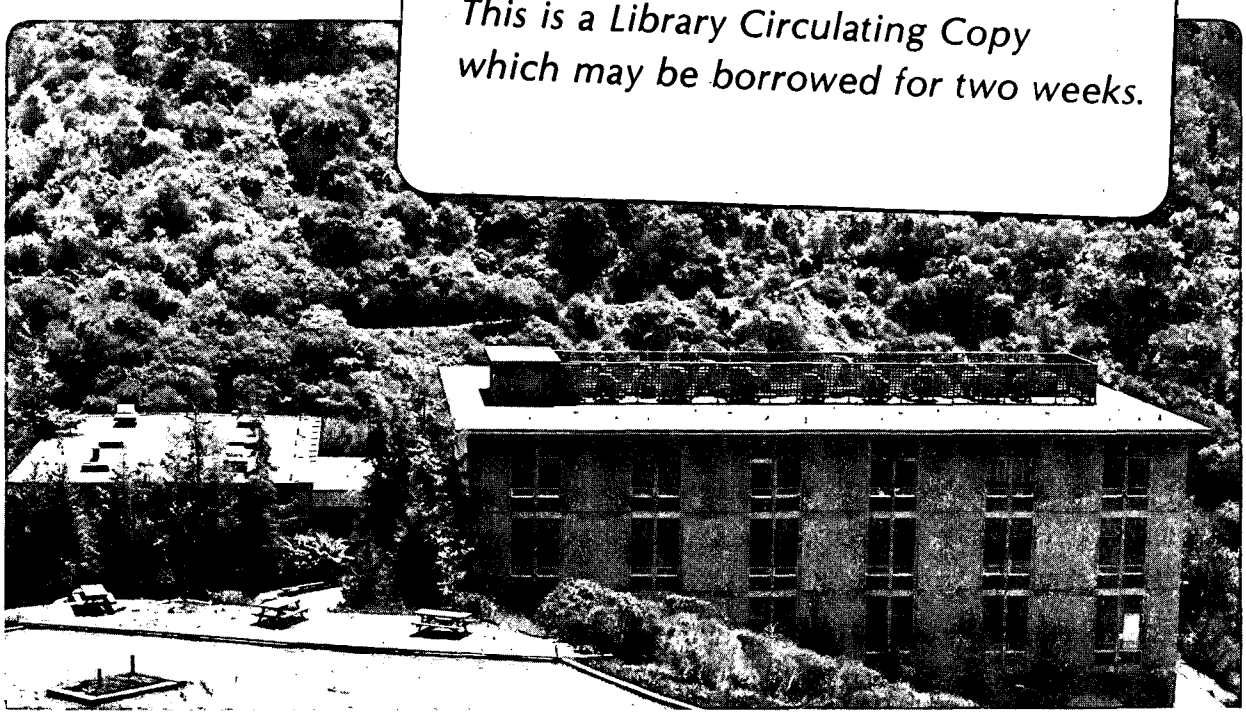

LBL-23058 c. 2

Prepared for the U.S. Department of Energy under Contract DE-AC03-76SF00098

DISCLAIMER

This document was prepared as an account of work sponsored by the United States Government. While this document is believed to contain correct information, neither the United States Government nor any agency thereof, nor the Regents of the University of California, nor any of their employees, makes any warranty, express or implied, or assumes any legal responsibility for the accuracy, completeness, or usefulness of any information, apparatus, product, or process disclosed, or represents that its use would not infringe privately owned rights. Reference herein to any specific commercial product, process, or service by its trade name, trademark, manufacturer, or otherwise, does not necessarily constitute or imply its endorsement, recommendation, or favoring by the United States Government or any agency thereof, or the Regents of the University of California. The views and opinions of authors expressed herein do not necessarily state or reflect those of the United States Government or any agency thereof or the Regents of the University of California.

The Preparation and Characterization of Rhenium Modified Pt(111) and Pt(100), and Platinum Modified Re(0001) Single Crystal Surfaces

David J. Godbey[†] and Gabor A. Somorjai

Department of Chemistry
University of California
Berkeley, California 94720
and
Materials and Chemical Sciences Division
Lawrence Berkeley Laboratory
Berkeley, California 94720

[†] Present address:

Chevron Research Company, P.O. Box 1627, Richmond, CA 94802

Abstract

Rhenium metal grows epitaxially on Pt(111) and Pt(100) in a layer by layer mode as shown by Auger electron spectroscopy and low energy electron diffraction. The growth mode of platinum metal on Re(0001) was also found to be layer by layer. Rhenium evaporated onto Pt(111) grows with a hexagonal close-packed structure exposing the (0001) face while on Pt(100) it grows with a face centered cubic structure exposing the (100) face. The surface composition of the bimetallic Re-Pt surface can be determined from the Auger spectrum when the coverage of rhenium is less than three monolayers.

Following rhenium deposition on platinum, chemical shifts were detected in the 4f levels of both adsorbate and substrate using XPS, and this is indicative of the formation of a surface alloy between the two metals. Annealing the bimetallic surface to 1150 K caused further shifts to higher binding energies for both the platinum and the rhenium 4f lines.

The presence of platinum on a partially oxidized Re(0001) surface was found to catalyze the decomposition of rhenium oxides under UHV and at a temperature as low as 400° C.

1 Introduction

Since the introduction of rhenium to the reforming catalyst in 1968 [1], many studies have been published aimed at understanding this complex system including those reported in references [2–26]. Most of these studies deal with the practical catalyst as a whole, consequently the information obtained from these studies cannot separate totally the metal–metal interaction from the influence of other variables.

For example, some questions still remain regarding the nature of the interaction between metals [8–17,26] , the oxidation state of the rhenium moiety in the active catalyst [2–7,9,14,15] , the effect of the alumina support on its activity [17,19,20], and the role of additives [12,18,21–25] . Most of the studies that have been reported, including the many surface science investigations, have focused on supported catalysts. In spite of the technological importance of this complex system, the dependence of the catalytic reforming activity and selectivity on the surface structure, alloy composition, and bonding of adsorbates, has not been adequately explored. The difficulty in separating the surface chemical and catalytic behavior of the metals from that of the high surface area oxide support introduces added complexity to the investigation of this already complex bimetallic system.

In order to explore the correlation of the surface composition and atomic structure with the catalytic activity of the metals, model surface and catalytic studies using single crystal surfaces of platinum, rhenium, and composite Pt–Re surfaces that were freshly prepared in ultra high vacuum have been initiated. Experiments were performed to help determine the nature of the metal-metal interaction between platinum and rhenium in the absence of an oxide support using both surface science and catalytic techniques. The results of the catalytic studies will be reported elsewhere.

In this paper is reported the preparation of bimetallic surfaces of rhenium on Pt(111) and Pt(100) by vapor deposition of rhenium metal onto platinum single crystal surfaces, and of platinum metal deposition onto Re(0001) single crystal surfaces. The composition and properties of the prepared bimetallic surfaces were characterized using Auger electron spectroscopy (AES), low energy electron diffraction (LEED), and X-ray photoelectron spectroscopy (XPS).

2 Experimental

Experiments using low energy electron diffraction and rhenium uptake using Auger electron spectroscopy were performed in a stainless steel ultra high vacuum (UHV) system pumped with a liquid nitrogen trapped diffusion pump; the base pressure obtained was 1×10^{-9} Torr after bakeout. The system was equipped with a four grid retarding field analyzer (RFA) used for LEED and AES, an ion gun for argon ion sputtering, and a quadrupole mass spectrometer. Auger electron spectra were obtained by operating the electron gun at an energy of 2 KeV and at a 90° angle to the axis of the RFA. The crystal was tilted 20° off normal from the RFA axis.

A second UHV chamber was used for the XPS study. This system was also pumped with a liquid nitrogen trapped diffusion pump, and the base pressure was better than 5×10^{-10} Torr following bakeout. This system was equipped with a double pass cylindrical mirror analyzer (CMA). X-rays were generated using a Mg Kα source. The substrate surface X-ray photoelectron signal was enhanced by tilting the Pt(111) crystal 50° off normal with respect to the CMA axis.

Platinum and rhenium single crystals were cut to within 1° of the desired orientations and both sides were polished using standard techniques. The area of the disks were about 1 cm^2 with a thickness of $\leq$0.5 mm. On the first chamber, the crystal was spot welded to platinum wires (0.020 in) which were spot welded to gold support rods (0.062 in.) affixed to a liquid nitrogen cooled block at the bottom of the manipulator. The mounting of the Pt(111) crystal was similar to the mounting on the first chamber except that tantalum rods replaced the gold supports, and the manipulator was equipped with X, Y, Z, tilt, and rotational motion.

In all cases resistive heating was used. Thermocouple wire pairs (0.005 in.)

were spot welded to the edge of the crystal. Chromel vs. alumel thermocouple was preferred due to the temperature calibration that exists between liquid nitrogen temperatures and 1700° C, and to the comparatively large millivolt intervals with the temperature scale (*e.g.* 25 K/millivolt). Chromel/alumel was used whenever platinum was employed. Rhenium can be heated to much higher temperatures, and in this case Pt vs. Pt–(10%)Rh thermocouple pairs were used.

Platinum and rhenium single crystals were cleaned by cycles of heating in oxygen ($\sim 3\times10^{-7}$ Torr) and argon ion sputtering (1×10^{-4} Torr Ar) at 1000 K with a 1 KeV argon ion beam energy, and annealing at 1300 K for platinum and 1600 K for rhenium until no impurities (mainly S, Ca, C, O) could be detected by AES or XPS. Rhenium was removed from platinum, and platinum removed from rhenium by prolonged argon ion sputtering (about 2 hours) at room temperature and 2 KeV primary beam energy after carbon had been removed in 3×10^{-7} Torr oxygen at 900 K. Following crystal cleaning, it was verified that sharp LEED patterns were obtained corresponding to a (1×1) for Pt(111) and Re(0001), and a (5×20) for the Pt(100) [27].

Rhenium metal was deposited from a 0.5 mm diameter filament resistively heated to 1800–2100 K. Platinum metal was deposited by heating to 1400–1700 K a 0.5 mm. diameter filament that was coiled about ten turns (the coil diameter was about 2 mm.). The condition of the filaments was monitored by checking the current required to just reach the visual threshold in a darkened room. As the filament deteriorated over a period weeks, the amount of current needed to reach this visual threshold decreased, hence the current needed to deposit metal at a given rate also decreased.

Deposition rates obtained were in the range of 2–8 minutes per monolayer (min/ML). The base pressure increased about fourfold, or to 4×10^{-9} Torr, after

about one minute of operation of the rhenium source at 5 min/ML. The increase in pressure observed was due to CO and CO_2 generated from the heating leads and tantalum shield of the source as it heated up. The rhenium source was allowed to cool after each minute of operation for about 30 seconds, and the platinum crystal was usually flashed to 700 K to remove any adsorbed CO or CO_2. When the deposition source was operated with platinum, no significant increase in temperature of the deposition source or in base pressure was observed. The platinum source has been operated for periods of over 30 minutes without requiring cool down.

The rhenium overlayer was oxidized for XPS experiments at room temperature and at 800 K with 2×10^{-7} Torr of oxygen for ten minutes. The oxidized overlayer was reduced in hydrogen at a pressure of 1×10^{-6} Torr and at 800 K for fifteen minutes. Following oxygen or hydrogen treatment, the sample was cooled to room temperature in the presence of the treatment gas. X-ray photoelectron measurements of the $4f_{7/2}$ lines of both platinum and rhenium were made at room temperature. The binding energies determined by XPS were accurate to ±0.3 eV.

3 Results

3.1 Rhenium Uptake on Pt(111) and Pt(100)

Rhenium uptake on Pt(111) was measured with AES using an RFA operated in the derivative mode. A plot of the platinum 158 eV peak intensity (the platinum 150 and 158 eV peaks were unresolved on this analyzer) versus time of rhenium deposition is shown in Figure 1. Breaks in the rhenium uptake curve near four and eight minutes correspond to the filling of the first and second monolayers respectively. After the filling of the third monolayer, the 158 eV platinum peak was no longer resolved above the secondary electron background due to the thickness

of the rhenium film. Representative spectra of some bimetallic surfaces derived from Pt(111) are shown in Figure 2.

The growth mechanism of rhenium on Pt(111) was found to be monolayer by monolayer at least through three monolayers. This was shown in Figure 1 by the presence of breaks in the Auger uptake curves of the platinum 158 eV peak at 4 and 8 minutes which is characteristic of a Frank-van der Merwe, or layer by layer growth mechanism. Adsorbate versus substrate plots gave the same information as the plot in Figure 1 and are not included here.

According to the Gallon model [28], for a given number of complete monolayers n of an adsorbate on a different substrate, the attenuation of the substrate signal is given by

$$I_s^{(n)} = \alpha^n \tag{1}$$

where $I_s^{(n)}$ is the signal from the substrate covered with n complete layers of adsorbate. α is defined by

$$\alpha = \frac{I_s^{(1)}}{I_s^{o}} \tag{2}$$

where I_s^{o} is the intensity of the clean substrate peak uncovered and $I_s^{(1)}$ is the intensity of the same peak covered with one monolayer of adsorbate. The adsorbate signal increases according to

$$I_a^{(n)} = I_a^{(\infty)} \left[1 - (1 - \frac{I_a^{(1)}}{I_a^{(\infty)}})^n \right] \tag{3}$$

where $I_a^{(n)}$ is the intensity of the Auger signal for n complete layers of adsorbate and $I_a^{(\infty)}$ is the intensity of bulk adsorbate. For an incomplete layer $n-1 < \theta_a < n$ where θ is the coverage in monolayers, the Auger signals for the substrate and the adsorbate is assumed to be a linear combination of the above expressions (Equations 1 and 3) for $n-1$ and n monolayers. The above model for the substrate behavior was plotted in Figure 1 for rhenium deposited on Pt(111) and gives good

agreement with experimental results. Further confirmation of layer by layer growth of rhenium on Pt(111) was that a well ordered (1×1) surface structure was always present during rhenium deposition on the Pt(111) crystal as shown by LEED and will be discussed later.

The inelastic mean free path (imfp) can be estimated from these data [27,28,29]. Assuming that the atomic backscattering coefficient is the same for platinum and rhenium (they are separated by osmium and iridium in the periodic table), then

$$\alpha = \exp(-d/0.75\lambda cos\phi) \tag{4}$$

where λ is the imfp, the factor 0.75 comes from the acceptance angle of the retarding field analyzer [29], d is the layer spacing, and ϕ is the photoelectron takeoff angle. Using $d = 2.23$ Å for rhenium, the imfp was calculated to be 3.5 Å, which is reasonable for 158 eV electrons [30].

It is important to be able to determine the coverage of an adsorbate by a single Auger spectrum. Platinum metal has a pair of Auger transitions near 158 eV, the 150 eV peak being unresolved on the analyzer used. Both platinum and rhenium metals have Auger transitions near 168 eV. As rhenium was deposited on platinum, the platinum 158 eV peak was attenuated, but the Pt + Re 168 eV peak intensity remained fairly constant up to 1.5 ML of rhenium. At larger rhenium coverages the 168 eV peak intensity increased. If the ratio of the intensities of the 158 and 168 eV peaks are plotted versus the rhenium coverage, linear behavior is observed through 2 monolayers of rhenium (Figure 3). The least squares line calculated from Figure 3 for the rhenium coverage through 2 monolayers was

$$\theta_{Re}(\pm 0.1 \text{ ML}) = (1.27 - I_{158}/I_{168})/0.56 \tag{5}$$

where I_{158} and I_{168} are the intensities of the 158 eV and 168 eV Auger peaks. The coverage of rhenium was assigned after deposition using the above equation and

the family of fingerprints like those shown in Figure 2. This method was also used by Sachtler to assign the composition of bimetallic gold–platinum surfaces [27].

Rhenium uptake was also measured on Pt(100). The uptake curves obtained were practically identical to those obtained from Pt(111), and are not included here (see Figure 1). The results obtained on Pt(100) indicate that a Frank-van der Merwe mechanism was also operating on this surface.

3.2 Platinum uptake on Re(0001)

Platinum uptake was measured on Re(0001) using the same chamber and configuration as for the rhenium uptake on platinum crystals. Since the platinum deposition source operated at a much lower temperature than the rhenium source, no increase in base pressure was observed and the bimetallic surfaces generated also remained cleaner. Platinum is more inert than rhenium and this also helped in keeping the surface clean of background gases. For these reasons it was not necessary to flash the bimetallic Pt–Re(0001) surface unless the preparation of alloyed surfaces was desired.

Uptake curves were obtained for platinum deposited on Re(0001) using Auger electron spectroscopy, and the results obtained are shown in Figure 4. The attenuation of the substrate rhenium 217 eV peak is reported for this system, but the growth of the adsorbate platinum 251 eV peak was also well behaved at low platinum coverages. This is in contrast to the rhenium on platinum system where no adsorbate rhenium peak could be measured quantitatively at coverages less than 0.5 monolayers.

The behavior of the adsorbate Pt 251 eV and the substrate Re 217 eV peaks were also modeled according to Gallon considering a layer by layer growth mechanism [28]. Equations 1 and 3 were used to generate the solid lines in Figure 4.

The model gives good agreement with the experimental data and is evidence that platinum growth on Re(0001) is layer by layer. This is in agreement with Alnot *et al.* who reported layer by layer growth of platinum on rhenium ribbon [31,32].

The attenuation coefficient of 217 eV electrons passing through one monolayer of platinum was calculated from these data to be $\alpha = 0.42$, and is very close to the value obtained for the attenuation coefficient of 160 eV electrons through rhenium. The value corresponds to an inelastic mean free path of 3.7 Å for 217 eV electrons through platinum as calculated using Equation 4, and is within the range obtained for 217 eV electrons propagating through other elements [30].

With the proceeding analysis complete, a set of Auger spectra were compiled that correspond to a given coverage of platinum on Re(0001). The ratio of many different peak combinations were calculated, and it was found that the ratio of the intensity of the Pt 251 eV peak divided by the intensity of the Pt + Re 168 eV peak versus coverage was well behaved up to at least 2 monolayers of platinum (Figure 5). The coverage of platinum on rhenium was estimated by calculating the ratio of intensities of the 251 eV and 168 eV peaks and reading the coverage from Figure 5. The Auger spectrum was also compared to the family of fingerprints obtained for the uptake curve of platinum on Re(0001) as was done for rhenium deposition on platinum crystals.

3.3 Stability of metallic thin films of platinum and rhenium

The rhenium overlayer was found to be stable on platinum up to 1000 K. Above these temperatures rhenium diffused into the platinum substrate. Flashing the surface to 1100–1300 K was hot enough to obtain mixing of the platinum and rhe-

nium metals in the interfacial region, and prolonged heating at these temperatures resulted in the eventual disappearance of rhenium, probably due to the diffusion of rhenium into the platinum bulk. Rhenium could also be removed from the platinum surface at 300° C in the presence of 300 Torr of oxygen, probably in the form of volatile Re_2O_7 as was reported previously [33].

Rhenium that was in contact with platinum metal resisted oxidation under vacuum conditions (10^{-7} Torr oxygen). Oxygen found on a Re–Pt(111) surface where the coverage of rhenium was $\theta_{Re} < 1$ ML could be removed by flashing the surface to 400° C without a change in the rhenium coverage, indicating that oxygen was not desorbing as a rhenium oxide. However, when depositing more than one monolayer of rhenium on platinum, contamination by small amounts of oxygen from the background gases, particularly from air and water, was difficult to avoid. There are two simple ways to remove oxygen from a rhenium surface in UHV. Heating to high temperatures ($\sim$ 2000 K) is one way, and the other is to chemisorb stoichiometric amounts of a molecule such as ethylene followed by flashing to 1000 K. Both methods cause bulk diffusion of the two metals, so a relatively thick rhenium film ($\sim$ 10 ML) must be deposited to insure that no platinum diffuses to the surface following annealing. For this reason it was difficult to control the surface oxygen coverage when attempting experiments at intermediate rhenium coverages such as 1 to several monolayers on platinum under vacuum conditions. However, experiments performed at elevated hydrogen pressures posed no difficulties because all rhenium films were found to reduce under atmospheric hydrogen pressures at 300° C, and Auger spectra obtained following these high pressure treatments showed no oxygen on the surface.

Platinum overlayers on rhenium were also found to be stable up to 1000 K. Above these temperatures platinum was lost from the surface by either diffusion

or by thermal desorption. Thermal desorption was not checked, but it does occur to some extent according to Alnot *et al.* [32]. Platinum could mostly be removed from rhenium by heating to high temperatures, although this is an undesirable method for removing a second metal from the surface since substantial accumulation may eventually develop in the near surface region. However, in the case of platinum on rhenium, it was difficult to remove the last monolayer of platinum with heating. One monolayer of platinum on rhenium remained on the surface for long periods of time, even at temperatures high above the diffusion threshold of the two metals. Alnot *et al.* also reported difficulties in removing the last half monolayer of platinum by heating to high temperatures [32].

The stability of a surface rhenium oxide was also tested in the presence of platinum. To remove oxygen from a monometallic rhenium surface, it was necessary to heat it in vacuum up to at least 2000 K. Experiments were performed in which oxygen was deliberately left on the rhenium surface. After dosing the rhenium surface with around 0.5 ML of platinum, the surface could be flashed free of oxygen at 400° C in vacuum. This indicates that platinum can catalyze the reduction of rhenium under UHV conditions by lowering oxygen desorption temperature. The catalyzed reduction of rhenium by platinum has been previously reported by investigators using temperature programmed reduction (TPR) of bimetallic supported platinum–rhenium catalysts [11,17], and the results obtained here show that the platinum catalyzed decomposition of rhenium oxides at lower temperatures may have been at least partially responsible for the enhanced reduction of rhenium in the presence of platinum.

The adsorbate induced surface segregation of rhenium oxides was also investigated. Experiments were performed where oxygen was chemisorbed on clean Re(0001) followed by the deposition of 10 monolayers of platinum. The Re(0001)

surface was dosed with oxygen until a (2×2) was observed using LEED indicating that the coverage of oxygen was $\theta_O \sim 0.25$ ML. After the deposition of platinum, the oxygen and rhenium were no longer detectable using AES. After a brief annealing of the surface to 800° C where the diffusion of platinum into rhenium is known to occur, both the rhenium and oxygen Auger signals reappeared with a decrease in the platinum Auger signal (Figure 6). Another brief annealing to 800° C resulted in an increased platinum Auger signal coupled to a decrease in the rhenium Auger signal, and disappearance of the oxygen signal. Further annealing to 800° C caused the platinum Auger signal to decrease as expected due to bulk diffusion of the metals. One interpretation of this effect is that rhenium oxide first segregated to the surface resulting in an increase in the rhenium and oxygen Auger signals. The increase in the platinum Auger signal observed following the second annealing resulted because the surface platinum catalyzed the reduction and desorption of oxygen from the surface-segregated rhenium oxide in vacuum. The presence of oxygen apparently led to surface segregation of the rhenium oxide because the surface free energy of the oxide was less than the surface free energy of both metallic platinum and rhenium. When the oxygen desorbed, the remaining metallic rhenium diffused from the surface to the near surface region leaving platinum layers on the surface resulting in a net decrease in surface free energy. It is also possible that once the surface segregation of the rhenium oxide occurred, further heating caused the desorption of the rhenium oxide as has been reported to occur by Philippart *et al.* [34].

3.4 XPS studies of the Re–Pt(111) system

X–ray photoelectron spectra were obtained of the Re–Pt(111) system. A reference spectrum of the clean Pt(111) 4f levels was obtained (Figure 7a), and all the

platinum and rhenium $4f_{7/2}$ lines subsequently measured were referenced to a Pt $4f_{7/2}$ binding energy at 70.9 eV [35].

The photoelectron spectrum obtained after 10 monolayers of rhenium were deposited is shown in Figure 7b. Assuming a value for the inelastic mean free path of 1200 eV electrons to be 18 Å [30], the thickness of the rhenium film was estimated by comparing the platinum XPS intensities before and after rhenium deposition. The crystal was flashed periodically to 700 K during the deposition of rhenium to keep the accumulation of carbon low. X–ray photoelectron spectra obtained following deposition and flashing to 700 K gave binding energies of 71.4 and 40.4 eV for the Pt and Re $4f_{7/2}$ levels respectively. This represents a shift to higher binding energy of 0.5 eV for the platinum $4f_{7/2}$ peak. The Pt $4f_{7/2}$ peak was also observed to widen at half maximum from 1.4 eV for clean platinum to 1.9 eV for rhenium covered platinum.

Following rhenium deposition and the above XPS measurement, the bimetallic surface was flashed to 1150 K and the results are shown in Figure 7c. This caused a change in the relative intensities of the platinum and rhenium 4f lines obtained by XPS which indicates that diffusion of rhenium into the platinum bulk and/or platinum diffusion into the rhenium surface layers had occurred. The thickness of the rhenium layer was estimated to be about 7 monolayers following flashing to 1150 K using Equation 4. The binding energies obtained were 71.8 and 40.8 eV for the platinum and rhenium $4f_{7/2}$ levels respectively. This represents a total shift toward higher binding energies of 0.9 eV for platinum, and 0.4 eV for rhenium compared to the clean metals.

The annealed bimetallic surface was exposed to oxygen at room temperature for 1 hour (Figure 7d), and at 800 K for 10 minutes (Figure 7e). A shoulder was observed to grow on the rhenium $4f_{7/2}$ peak centered about 1 eV higher in

binding energy than the parent peak following the oxygen treatment at 800 K. This shoulder was attenuated almost completely after treating with 1×10^{-6} Torr hydrogen at 800 K (Figure 7f). A summary of the XPS results is shown in Table 1.

3.5 Structure of rhenium multilayers on Pt(111)

The LEED pattern generated following the deposition of any amount of rhenium on Pt(111) was always due to a (1×1) surface structure (Figure 8). This was the case even when 5–10 monolayers of rhenium were deposited and the platinum substrate could not be detected using AES. However, symmetry differences were observed when scanning the electron beam energy in the range of 50–200 eV. LEED spots of equivalent symmetry change intensity together when the electron beam energy is changed. Six–fold symmetry is shown by all six spots changing intensity together, while three–fold symmetry is shown by the two different sets of symmetry related spots changing intensity together as shown in Figure 8.

If the observed differences are caused by the formation of a different crystal structure, it is possible to distinguish between a hexagonal close-packed hcp(0001) and a face-centered cubic fcc(111) surface. The escape depth of 50–200 eV electrons is on the order of two atomic layers, so LEED experiments should show three-fold symmetry for both the ideal fcc(111) and hcp(0001) surfaces. However, no surface is perfect and defects in the form of steps are present on the surface. If a step with the height of a single atom is considered on an fcc(111) surface, it can be seen that the surface unit cell is unchanged in moving across the step due to the *abcabc* packing of the fcc system. The LEED pattern obtained from either domain is indistinguishable, and three-fold symmetry is observed (Figure 8). However, the surface unit cell for the hcp(0001) surface is rotated 60° upon moving

across the monatomic step due to the *ababab* packing of the hcp system. Since these two domains exist on the imperfect hcp(0001) surface, the LEED pattern is a superposition of the patterns produced by both domains, and six fold symmetry results by averaging unequal spot intensities (Figure 8) [36].

For the rhenium on Pt(111) system, rhenium was found to grow with an hcp structure exposing the (0001) face. This was shown by LEED because six-fold symmetry was observed when multilayers (>5 ML) of rhenium were present on the surface while three-fold symmetry was observed for clean Pt(111) [36]. These results are in agreement with those found by Zaera and Somorjai [37,38]. Intermediate structures were not analyzed, and it is not known whether rhenium fills the fcc or hcp hollow of the surface during deposition of the first and second monolayers.

3.6 Structure of rhenium multilayers on Pt(100)

Clean Pt(100) reconstructs to yield a (5×20) surface structure. This structure has been interpreted as an hexagonal surface layer resting on a second layer with the characteristic (1×1) square lattice (Figure 9a) [39,40,41]. The reconstruction can be removed by carefully leaking CO into the chamber while watching the LEED pattern change, and in this manner conversion from a (5×20) to a (1×1) surface structure was observed (Figure 9b). The (5×20) restructured surface could be regenerated by flashing the crystal to 800 K which removed the adsorbed CO. The deposition of rhenium onto the Pt(100) surface also removed the (5×20) surface structure. The observed conversion to the (1×1) structure began near 0.15 ML of rhenium and was completed near 0.3 ML. The (5×20) structure was not regenerated by flashing to 900 K indicating that rhenium and not CO was responsible for the structural transformation. This phenomenon has been reported

previously where copper was observed to remove the (5×20) reconstruction of Pt(100) [42].

As more rhenium was deposited on this surface, a (1×1) surface structure was continually observed, but the diffuse background intensity increased. At coverages between 0.3 and ten monolayers of rhenium, a (1×1) structure was always discernible over the diffuse background, even though no platinum could be detected using AES. Flashing the surface briefly to 1300 K caused some rhenium to diffuse into the platinum substrate. Even though AES showed no trace of the underlying platinum substrate, the LEED pattern was observed to sharpen considerably with no extra spots appearing (Figure 9c). The interatomic distances for pure platinum and rhenium differ by only about 1% (2.77 and 2.74 Å respectively), and it was not possible to determine whether the interatomic distance obtained for the rhenium overlayer on Pt(100) was platinum- or rhenium-like. Indeed, an analysis of the spot to spot distance generated by the rhenium covered Pt(100) and the Pt(100) (1×1) (Figure 9b) showed the interatomic distance to be indistinguishable within experimental error. Since the hexagonal close-packed system does not have a surface analogous to the fcc(100) surface, it is concluded that rhenium grows face-centered cubic on Pt(100).

An additional feature observed in the rhenium covered surface was the faint lines connecting the spots (Figure 9c), and is evidence that strain was present along preferred orientations in the rhenium overlayer.

3.7 Platinum multilayers on Re(0001)

The LEED pattern generated by a Re(0001) surface is due to a (1×1) surface structure and displays 6 fold symmetry since rhenium is an hcp metal as discussed in Section 3.5. Platinum grows layer by layer on the Re(0001) surface, but the

well ordered LEED pattern generated by the clean rhenium surface disappears as platinum deposition proceeds. At 15 layers of platinum the diffuse background observed was high indicating a high degree of disorder.

Annealing the surface briefly to 100° C caused no change in the disorder observed. Annealing the surface briefly to 200° C did cause spots to appear although still somewhat diffuse. The symmetry that was observed appeared to be identical to the symmetry observed on the clean Re(0001) substrate (Figure 8). A brief annealing to 300° C sharpened the LEED spots considerably, and the six–fold symmetry was confirmed. This surprising result indicates that platinum may form a hexagonal close-packed film on Re(0001) exposing the (0001) face.

4 Discussion

4.1 Stuctures and growth mechanisms

Rhenium grows ordered on platinum with an interatomic distance indistinguishable from both the pure platinum and the pure rhenium interatomic distances (the interatomic distances of the two metals are within 1% of each other). On Pt(111) a well ordered LEED pattern corresponding to a (1×1) surface structure was always observed. The six fold symmetry observed when 10 ML of rhenium was deposited indicates an hcp rhenium structure grows on Pt(111). For rhenium growing on Pt(100) the situation is somewhat different. Since the hcp system has no surface with a square unit cell, rhenium is forced to grow fcc on Pt(100), and remains fcc through at least 10 ML. Strain did exist in the rhenium overlayer on Pt(100) and was evident by the lines connecting the substrate spots shown in Figure 9c. This strain was probably caused by the lattice mismatch between platinum and rhenium, and because the rhenium film was forced to grow in an

unfavorable crystal structure. Similar behavior was observed for cobalt growing on Cu(100) by Salmerón *et al.* as they presented evidence for the formation of fcc cobalt [43]. The fcc growth of rhenium on Pt(100) can be explained as a template effect. Since rhenium can grow fcc on Pt(100) indicates that the free energy associated with the fcc crystal structure is not too much larger than the free energy of the hcp crystal structure for rhenium. An inspection of the phase diagram for the rhenium-platinum system cannot explain this, however. Platinum and rhenium form a paratectic binary system, and the phase diagram shows that on the platinum rich side an fcc solid solution exists and an hcp solid solution exists on the rhenium rich side with a two phase region between 40–60 % rhenium. However, AES showed that the upper three layers were devoid of platinum while LEED showed the existence of fcc rhenium layers. Apparently a template effect is strong enough to support fcc rhenium for many monolayers.

The apparent growth of platinum films on Re(0001) in an hexagonal close-packed film is not easy to explain. The hexagonal close-packed and face-centered cubic systems do have a common face; the exposed atomic layer of the hcp(0001) surface has the same structure as the exposed atomic layer of the fcc(111) surface. Rhenium growing hcp on Pt(111) is perhaps not surprising since the rhenium film can grow in its natural crystal structure using the Pt(111) surface as a template. With platinum deposition on Re(0001) a different picture emerges. Platinum grows disordered on this surface as shown by the loss of the LEED pattern during platinum deposition, even though using AES proved that it grows layer by layer. Annealing the surface to 300° C was high enough to attain an ordered surface structure, but not high enough to cause bulk diffusion which required temperatures in excess of 700° C. Therefore if platinum does grow hcp on Re(0001), then a long range interaction between the two metals must exist because the difference between

the fcc structure and the hcp structure as viewed through their basal planes is not manifest until the third layer. The rhenium metal substrate was apparently able to perturb the platinum overlayer and cause it to form an hcp structure through at least 10–15 monolayers. Confirmation of the growth of hcp platinum on Re(0001) using LEED I(V) analysis would be useful, but has not yet been performed.

Comments are also in order regarding the growth mechanism observed for rhenium on platinum. Sachtler *et al.* observed that gold grows layer by layer on platinum substrates, but that platinum forms three dimensional crystallites on gold substrates [27]. This is reasonable because the surface free energy of gold is lower than that of platinum as calculated by the method of Tyson and Miller (1.48 and 2.46 J/m^2 for Au and Pt respectively) [44]. Using the above surface free energy argument, platinum should grow layer by layer on rhenium as was observed experimentally, but rhenium should form three dimensional crystallites on platinum (3.61 J/m^2 was calculated for the surface free energy of rhenium from reference [44]). Since rhenium also grows layer by layer on platinum, there must be forces operating of sufficient strength to overcome the differences in the surface free energies of the two components. An explanation invoking a lattice mismatch is not satisfactory because the difference in nearest neighbor distance of platinum and rhenium is small at 1% (2.77 Å and 2.74 Å for Pt and Re respectively). A more plausible explanation invokes the formation of relatively strong Pt–Re bonds and a surface alloy.

4.2 Alloy formation in bimetallic Pt–Re surfaces

The formation of a surface alloy is also supported by XPS results. Following deposition of a 10 ML film of rhenium on Pt(111), the binding energy for the platinum $4f_{7/2}$ line was found to increase relative to clean platinum. The magnitude

of this shift in the presence of epitaxial rhenium was 0.5 eV for the platinum $4f_{7/2}$ peak and is similar to the shift reported in the literature for supported and unsupported alloyed systems [10,18,31,32].

It is somewhat surprising that a 0.5 eV shift was observed for the platinum substrate in the presence of *epitaxial* rhenium overlayers. Although the XPS signal generated by the platinum layer in contact with a rhenium layer might be expected to experience such a shift, the bulk unperturbed platinum underneath this layer should dominate the XPS signal resulting in a small, if any, observed shift. Frequent checks against a gold foil attached to the back side of the manipulator revealed that the energy calibration of the spectrometer was not drifting. A possible cause of the platinum shift was that mixing of platinum and rhenium in the interfacial region occurred leading to an enhancement with respect to the bulk platinum signal of the interfacial platinum signal under the 20–30 Å rhenium overlayer. Temperatures high enough to lead to mixing in the interfacial region was provided by the flashing to 700 K at intervals during the rhenium deposition, even though it was shown that significant bulk diffusion did not occur at this temperature. The broadening of the Pt $4f_{7/2}$ peak may also have been caused by this alloying effect, and the broadness of the signal observed can be explained by the contribution to the platinum signal from a mixture of many $PtRe_x$ species, including a contribution from the underlying bulk platinum substrate. The reason that Tysoe *et al.* failed to observe a shift in the platinum $4f_{7/2}$ peak must be due to the difference in preparation of the bimetallic surfaces [33]. They did not flash the surface during rhenium deposition and consequently may have accumulated carbon in the rhenium film.

After annealing the bimetallic surface to higher temperatures (1150 K), a further increase in binding energy of the 4f levels of platinum, and an increase in

binding energy of the rhenium 4f levels were observed. At these temperatures, significant mixing of the two metals had occurred as shown by the change in peak intensities of the platinum and rhenium components. The binding energy increase for platinum and rhenium was 0.9 and 0.4 eV respectively compared to the clean metals. Similar results were obtained by Alnot *et al.* who evaporated platinum on rhenium ribbon [32]. They reported a Pt $4f_{7/2}$ binding energy of 71.6 eV at low coverages (<0.5 ML) which decreased to 71.1 eV at three monolayers of platinum. They also report that annealing a thick platinum deposit ($\sim$ 70 ML) on rhenium ribbon to 1400 K gave binding energy shifts to higher binding energies of 1 and 0.6 eV for the platinum and rhenium $4f_{7/2}$ peaks respectively (relative to the clean metals), with an increase in the full width at half maximum (fwhm) for the platinum peak of 0.3 eV. The increase in width of the Pt $4f_{7/2}$ peak observed in this study was 0.5 eV when 10 layers of rhenium were deposited on Pt(111). The shift to higher binding energy of the $4f_{7/2}$ peaks for both platinum and rhenium was also observed for SiO_2 supported Pt–Re catalysts by Biloen *et al.* [18].

4.3 Oxidation and reduction of bimetallic surfaces

The oxidation and reduction of rhenium in an alloyed platinum–rhenium surface under vacuum conditions was also examined using XPS. The bimetallic alloyed surface could be partially oxidized only at elevated temperatures ($\geq$ 800 K). It is possible that longer exposure to 3×10^{-7} Torr of oxygen would oxidize the underlying bulk rhenium more completely. However, results obtained by Zaera [37] and Tysoe *et al.* [33] indicate that higher pressures of oxygen are needed to cause a complete shift in the peak position of the Re $4f_{7/2}$ peak. Comparison to the results obtained by Tysoe *et al.* suggest that after high temperature oxidation of the alloyed surface, the shoulder observed at higher binding energies was due to an

oxidized rhenium species. The peak position of this shoulder was located between the peak positions determined for ReO (Re^{2+}) and ReO_2 (Re^{4+}) determined by Zaera who measured the chemical shifts observed towards higher binding energies relative to rhenium metal of $\sim$ 1 and 2 eV respectively for ReO and ReO_2 [37].

Platinum has been observed previously to catalyze the reduction of rhenium, and the catalyzed reduction of rhenium by platinum reported from TPR studies has been attributed to migration over the support by either hydrated rhenium oxides to platinum reduction centers, or of activated hydrogen [11,17]. In the case of activated hydrogen, hydrogen can be activated with dissociation on platinum metal, followed by hydrogen spillover onto the support with migration to the rhenium oxide particles which can then be reduced [45]. Although the migration of hydrogen under high pressure conditions may be important, it was shown that platinum catalyzes the desorption of oxygen from rhenium in vacuum. This means that platinum catalyzes the decomposition of rhenium oxides to metal and O_2 under mild conditions, *i.e.* at temperatures near 400° C as follows

$$ReO_x \xrightarrow{Pt} Re + \frac{x}{2}O_2$$

Under industrial conditions this would probably result in the sticking together of the Pt and Re species to form the nucleus of a bimetallic particle when a migrating ReO_x species encounters a metallic reduction center. This mechanism may also be operating at higher temperatures, although it is possible that at temperatures near 700° C the loss of oxygen was due to the desorption of rhenium oxides as was reported to occur by Philippart *et al.*.

5 Conclusions

A moderately strong interaction between platinum and rhenium metals has been shown to exist, and is supported by the following results. Rhenium grows ordered and layer by layer on Pt(111) and Pt(100), and even forms an fcc structure on Pt(100). Platinum grows layer by layer on the Re(0001) surface and possibly forms a hexagonal close-packed structure. A surface alloy was observed to form between the two metals at 700 K and is shown by XPS both by the broadening of the Pt $4f_{7/2}$ peak in the presence of rhenium, and by the chemical shifts observed for the Re and Pt $4f_{7/2}$ peaks following vapor deposition and annealing of rhenium films on Pt(111). The presence of platinum on a rhenium surface facilitates the decomposition of rhenium oxides and subsequent desorption of oxygen under UHV at temperatures much lower than would be possible from monometallic rhenium.

Acknowledgment

This work was supported by the Director, Office of Energy Research, Office of Basic Energy Sciences, Materials Sciences Division of the U.S. Department of Energy under contract DE-AC03-76SF00098. We would like to acknowledge Gerard Vurens for his assistance with the X-ray photoelectron experiments, and to Miguel Salmerón for his helpful discussions.

References

[1] H. E. Kluksdahl. *U. S..Patent 3,415,737* (1968) .

[2] A. N. Webb. *J. Catalysis* **39** (1975) 485.

[3] M. F. L. Johnson and V. M. LeRoy. *J. Catalysis* **35** (1974) 434.

[4] H.C. Yao and M. Shelef. *J. Catalysis* **44** (1976) 392.

[5] L. Wang and W.K. Hall. *J. Catalysis* **82** (1983) 177.

[6] E.S. Shapiro, V.I. Avaev, G.V. Autoshin, M.A. Ryashentseva, and K.M. Minachev. *J. Catalysis* **55** (1978) 402.

[7] M.F.L. Johnson. *J. Catalysis* **39** (1975) 487.

[8] J.B. Peri. *J. Catalysis* **52** (1978) 144.

[9] H. Charcosett, R. Frety, G Leclercq, E. Mendes, M. Primet, and L. Tournayan. *J. Catalysis* **56** (1979) 468.

[10] M. Alnot, A. Cassuto, R. Ducros, J.J.Ehrhardt, and B. Weber. *Surface Sci.* **114** (1982) L48.

[11] B.H. Isaacs and E.E. Petersen. *J. Catalysis* **77** (1982) 43.

[12] J.M. Parera, C.A. Querini J.N. Beltramini, E.E. Martinelli, E.J. Churin, P.E. Aloe, and N.S. Figoli. *J. Catalysis* **99** (1986) 39.

[13] C. Betizeau, G. Leclercq, R. Maurel, C. Bolivar, H. Charcosset, R. Fretty, and L. Tourayan. *J. Catalysis* **45** (1976) 179.

[14] J.H. Onuferko, D.R. Short, and M.J. Kelley. *Appl. of Surface Sci.* **19** (1984) 227.

[15] D.R. Short, S.M. Khalid, J.R.Katzer, and M.J. Kelley. *J. Catalysis* **72** (1981) 288.

[16] R.J. Bertolacinni and R.J. Pellet. *Catalyst Deactivation*, pages 73–77. Elsevier, Amsterdam, The Netherlands, 1980.

[17] R.L. Mieville. *J. Catalysis* **87** (1984) 437.

[18] P. Biloen, J.N. Helle, H. Verbeek, F.M. Dautzenberg, and W.M.H. Sachtler. *J. Catalysis* **63** (1980) 112.

[19] J. Margitfalvi, S. Gőbölös, E. Kwayzer, M. Hegedüs, F. Nagy, and L. Koltai. *React. Kinet. Catal. Lett.* **24** (1984) 315.

[20] V. Eskinazi. *Applied Catalysis* **4** (1982) 37.

[21] R.W. Coughlin, A. Hasan, and K. Kawakami. *J. Catalysis* **88** (1984) 163.

[22] V.K. Shum, J.B. Butt, and W.M.H. Sachtler. *J. Catalysis* **99** (1986) 126.

[23] V.K. Shum, J.B. Butt, and W.M.H. Sachtler. *J. Catalysis* **96** (1985) 371.

[24] M.A. Pacheco and E.E. Petersen. *J. Catalysis* **96** (1985) 507.

[25] C.R. Apestequía and J. Barbier. *J. Catalysis* **78** (1982) 352.

[26] J. Barbier, H. Charcosset, G. dePeriera, and J. Riviere. *Applied Catalysis* **1** (1981) 71.

[27] J.W.A. Sachtler, M.A. Van Hove, J.P. Biberian, and G.A. Somorjai. *Surface Sci.* **110** (1981) 19.

[28] T.E. Gallon. *Surface Sci.* **17** (1969) 486.

[29] M.P. Seah. *Surface Sci.* **32** (1972) 703.

[30] G. Ertl and J. Küppers. *Low Energy Electrons and Surface Chemistry.* Verlag–Chemie, Weinheim, Germany, 1974.

[31] M. Alnot, V. Gorodetskii, A. Cassuto, and J.J. Ehrhardt. *Surface Sci.* **162** (1985) 886.

[32] M. Alnot, A. Cassuto, J.J. Ehrhardt A. Slavin, and B. Weber. *Appl. of Surface Sci.* **10** (1982) 85.

[33] W.T. Tysoe, F. Zaera, and G.A. Somorjai. *Surface Sci.* (1987) Submitted.

[34] J.L. Philippart, B. Weber, and A. Cassuto. *Appl. of Surface Sci.* **10** (1982) 21.

[35] C.D. Wagner, W.M. Riggs, L.E. Davis, J.F. Moulder, and G.E. Muilenberg (editor). *Handbook of X-Ray Photoelectron Spectroscopy.* Perkin-Elmer Corporation, 1979.

[36] H.L. Davis and D.M. Zehner. *Bull. Am. Phys. Soc.* **24** (1979) 468.

[37] F. Zaera. PhD thesis, University of California, Berkeley, CA 94720, 1984.

[38] F. Zaera and G.A. Somorjai. *Surface Sci.* **154** (1985) 303.

[39] M.A. Van Hove, R.J. Koestner, P.C. Stair, J.P. Biberian, L.L. Kesmodel, I. Barton, and G.A. Somorjai. *Surface Sci.* **103** (1981) 189.

[40] D.G. Fedak and N.A. Gjostein. *Surface Sci.* **8** (1967) 77.

[41] P.W. Palmberg and T.N. Rhodin. *J. Chem. Phys.* **49** (1968) 134.

[42] C.J. Barnes, M. Lindroos, and M. Pessa. *Surface Sci.* **152/153** (1985) 260.

[43] L. González, R. Miranda, M. Salmerón, J.A. Vergés, and F. Ynduráin. *Phys. Rev. B* **24** (1981) 3245.

[44] W.R. Tyson and W.A. Miller. *Surface Sci.* **62** (1977) 267.

[45] R. Lamartine and R. Perrin. *Spillover of Adsorbed Species*, page 251. Elsevier Science Publishers, Amsterdam, The Netherlands, 1983.

Table 1: XPS Binding Energies in eV (±0.3 eV).

Treatment	Pt $4f_{7/2}$	Re $4f_{7/2}$
Clean Pt[a]	70.9	—
10 ML Re	71.4	40.4
Anneal to 1150 K	71.8	40.8
Oxidize 800 K	71.8	42[b]
Reduce 800 K	71.7	40.7

a. Reference [35]
b. High binding energy shoulder.

Captions for figures

Figure 1: Rhenium uptake on Pt(111). Breaks near four and eight minutes correspond to the filling of the first and second monolayers of Re. The solid lines were generated by the Gallon model for layer by layer growth. A similar plot was obtained for rhenium uptake on Pt(100).

Figure 2: Representative Auger spectra obtained of Re on Pt(111). Shown are spectra for clean Pt, and $\theta_{Re} = 1$, 2, and 3 monolayers on Pt(111) respectively.

Figure 3: Ratio of the Auger 158 eV peak to the 168 eV peak obtained during Re uptake on Pt(111) and Pt(100).

Figure 4: Platinum uptake on Re(0001) monitoring the adsorbate Pt 251 eV (o) and the substrate Re 217 eV peak (•). The solid lines were generated by the Gallon model for layer by layer growth.

Figure 5: Ratio of the AES 251 eV to the 168 eV peak vs. coverage for platinum dosed Re(0001).

Figure 6: Diffusion of rhenium oxides through platinum metallic overlayers as shown by AES. The upper panels show the region 100–300 eV. Notice the behavior of the Pt 150 and 155 eV peaks. The lower panels show the oxygen region. a) Clean Re foil. b) After 10 ML Pt. c) After flashing to 800° C. d) After a second flashing to 800° C. e) After flashing to 850° C.

Figure 7: Normalized X–ray photoelectron spectra obtained from Re modified Pt(111) were recorded at room temperature. a) Clean Pt(111). b) After deposition of 10 ML of Re. c) Anneal surface from b to 1150 K. d) Surface from c treated in 2×10^{-7} Torr O_2 at room temperature. e) Surface from d heated to 800 K in 2×10^{-7} Torr O_2. f) Surface from e heated to 800 K in 1×10^{-6} Torr H_2.

Figure 8: Reciprocal and real space representations of fcc(111) and hcp(0001) surfaces. For Pt(111), two equivalent sets of spots with 3-fold symmetry are indicated as solid or open spots. For Re(0001), all six spots are equivalent. Below the LEED patterns are shown schematic representations of real space surfaces with a single monatomic step for fcc(111) and hcp(0001) surfaces.

Figure 9: Evidence for the formation of face-centered cubic Re on Pt(100) surface. (a) Top panel. (b) Middle panel. (c) Bottom panel.

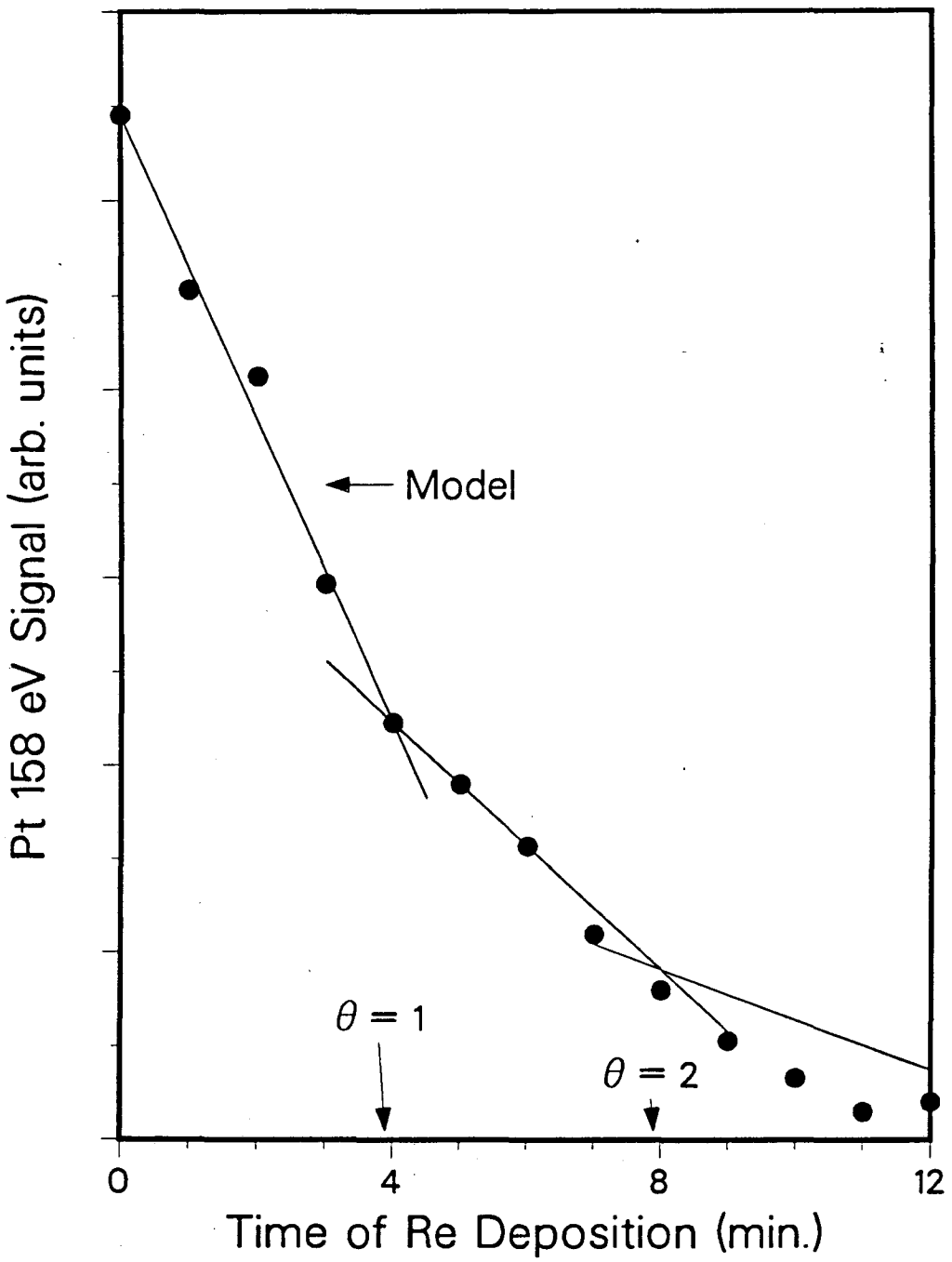

XBL 8711-4586

Fig. 1

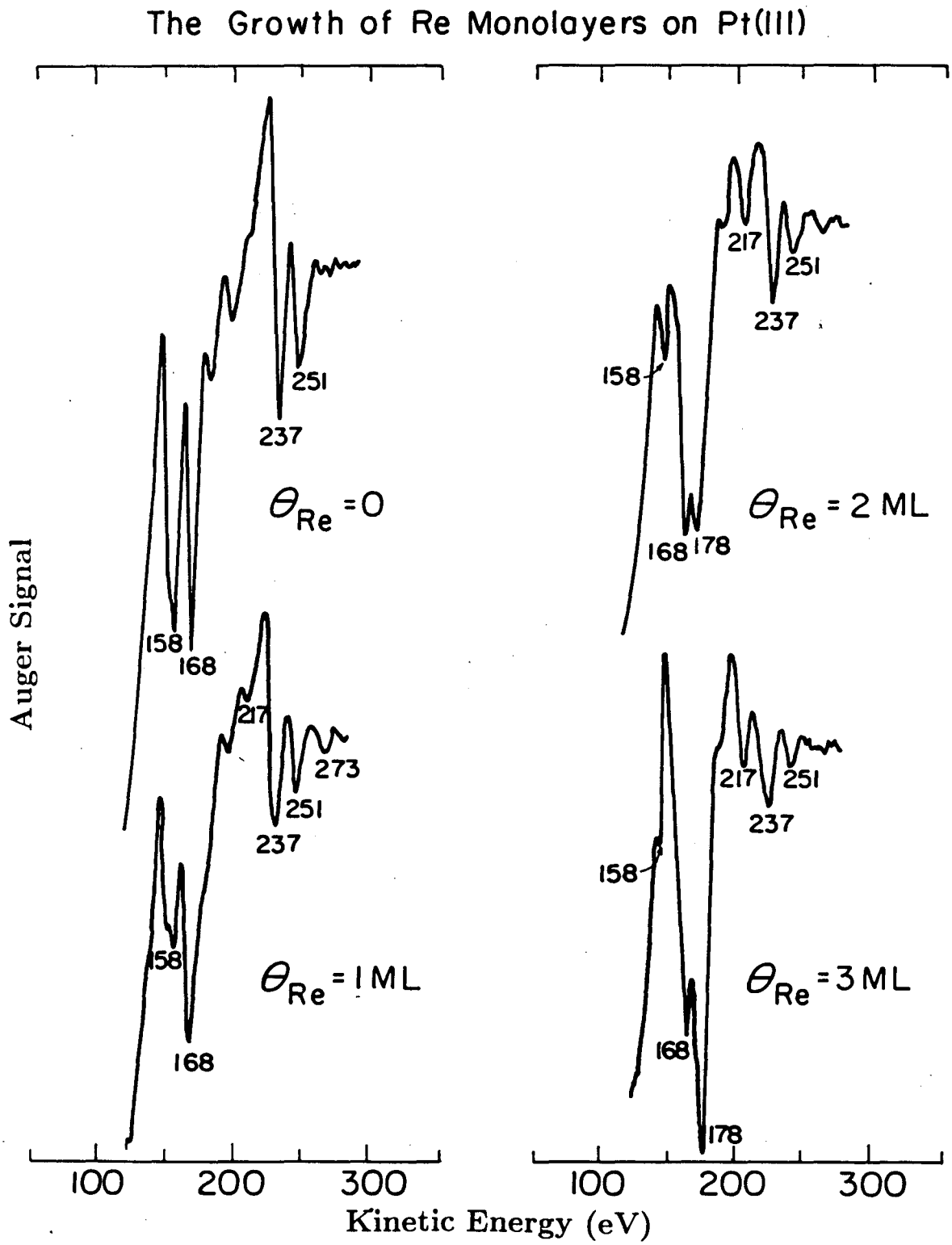

XBL 8711-4583

Fig. 2

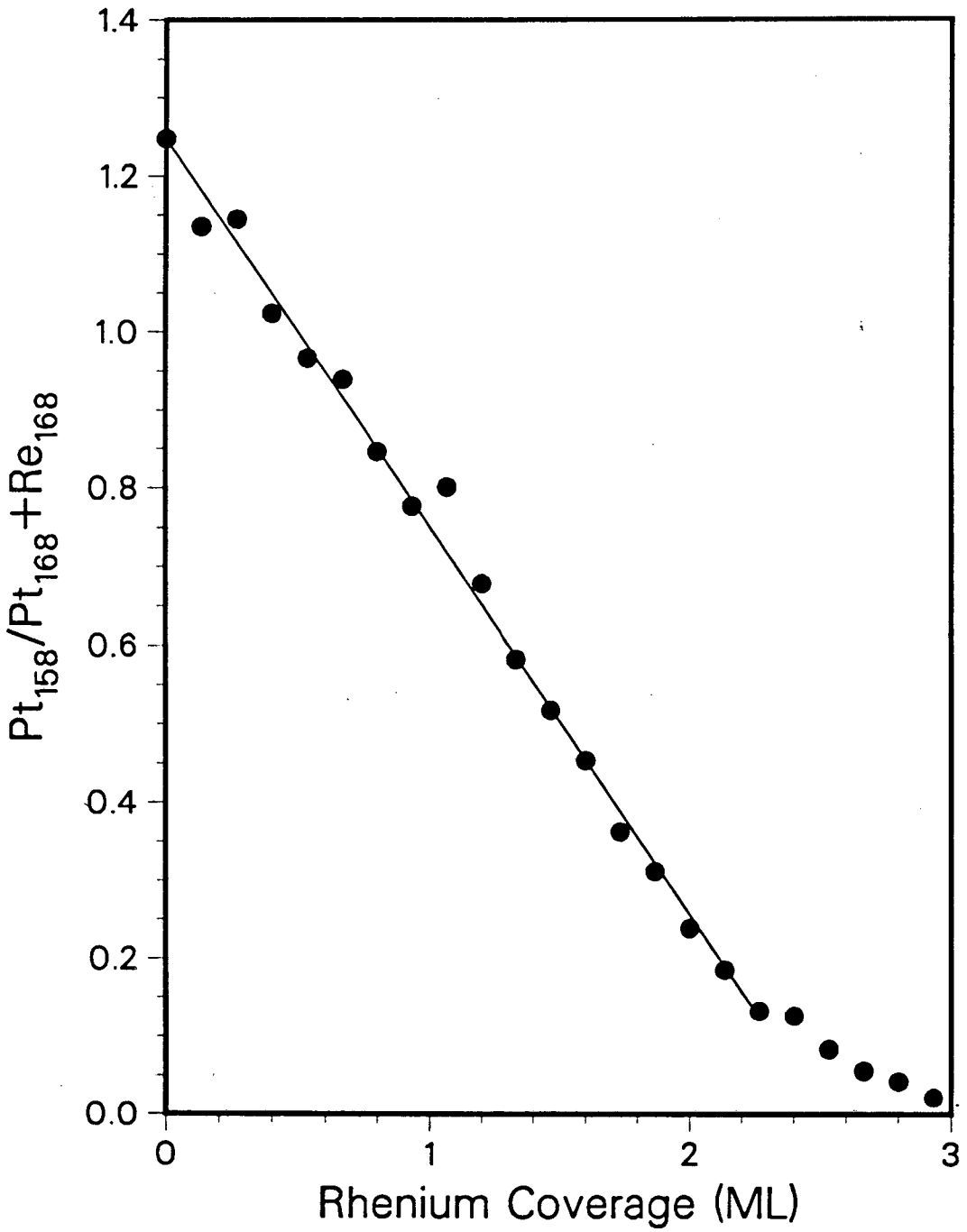

XBL 8711-4587

Fig. 3

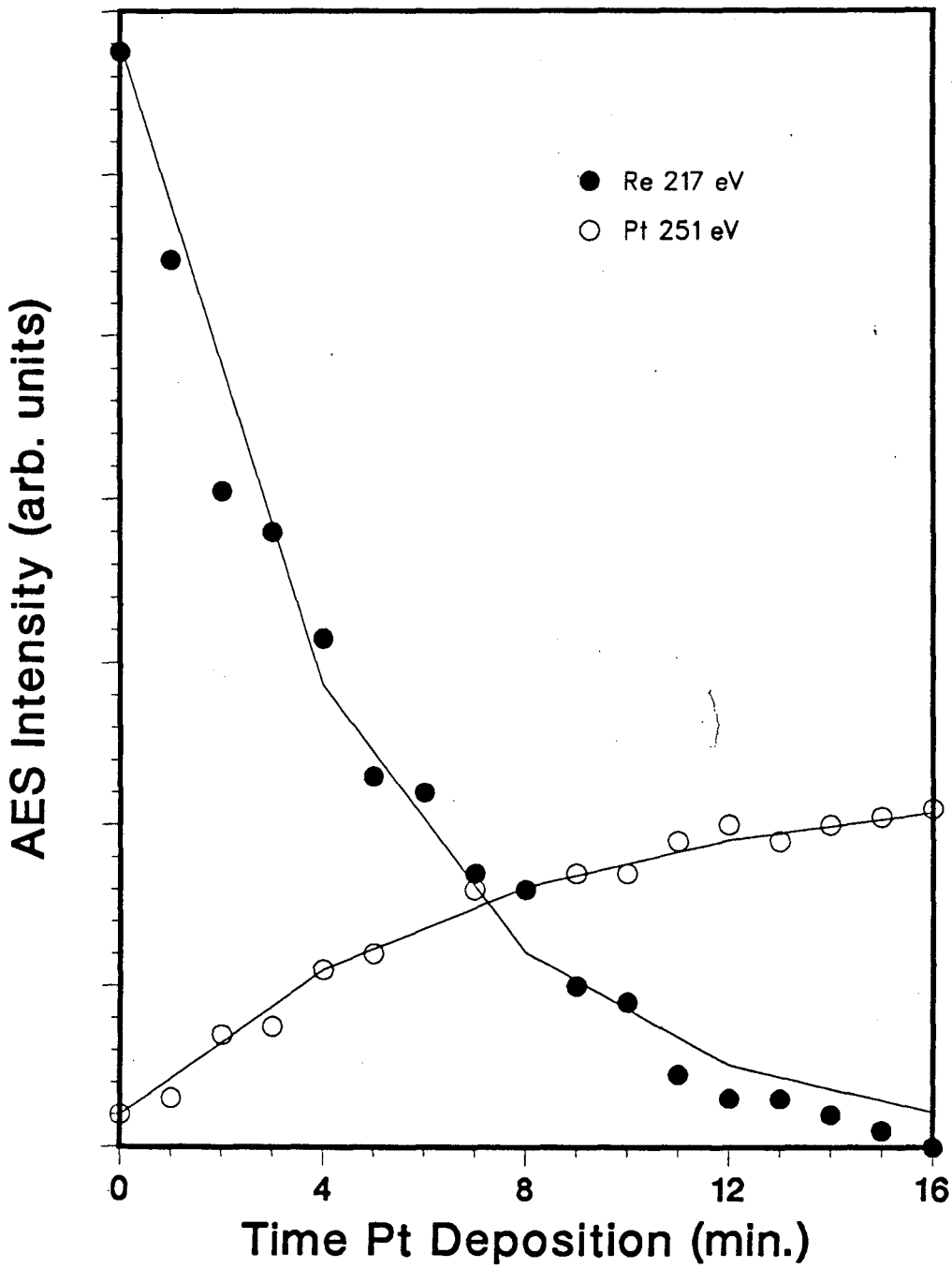

XBL 8711-4584

Fig. 4

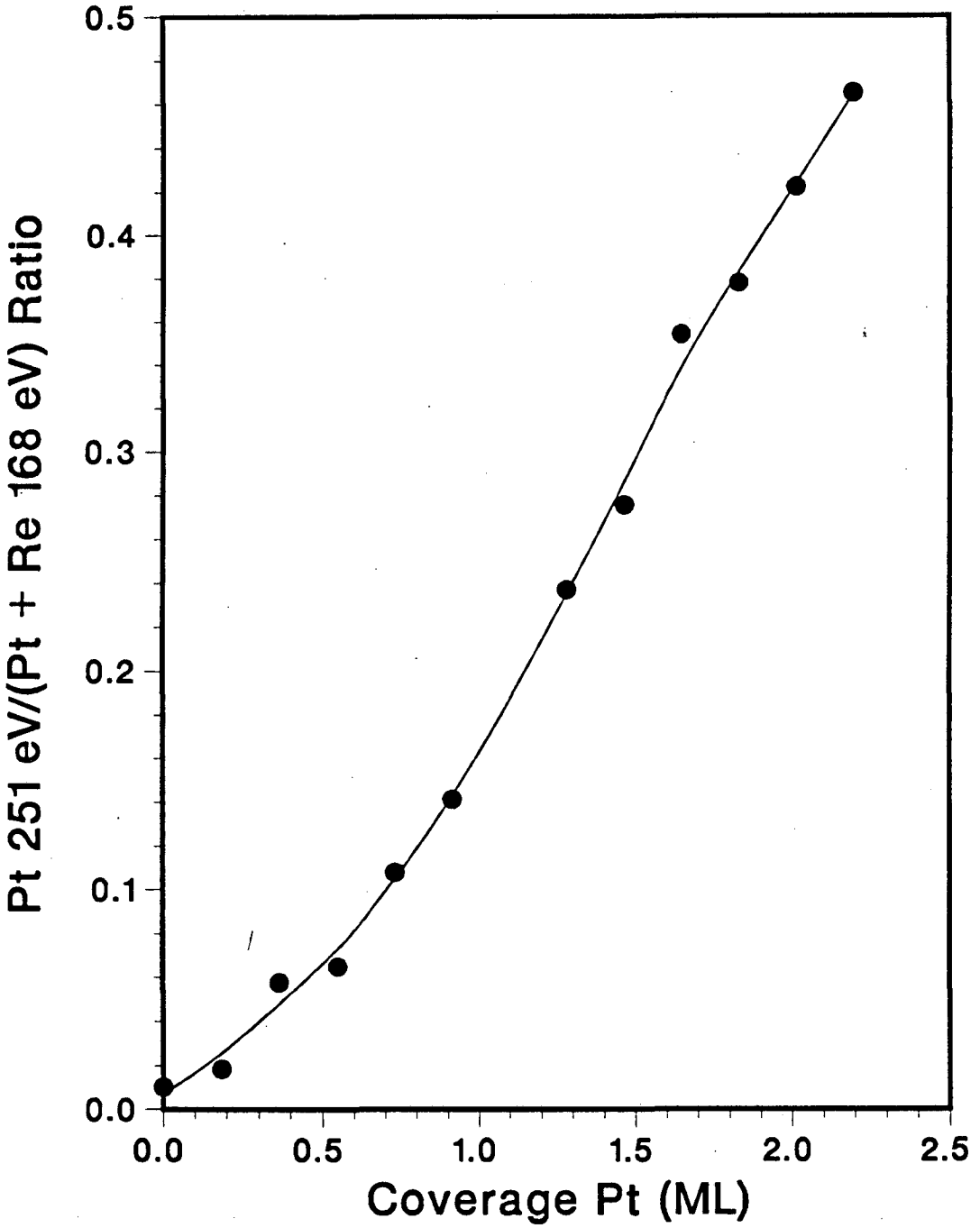

XBL 8711-4585

Fig. 5

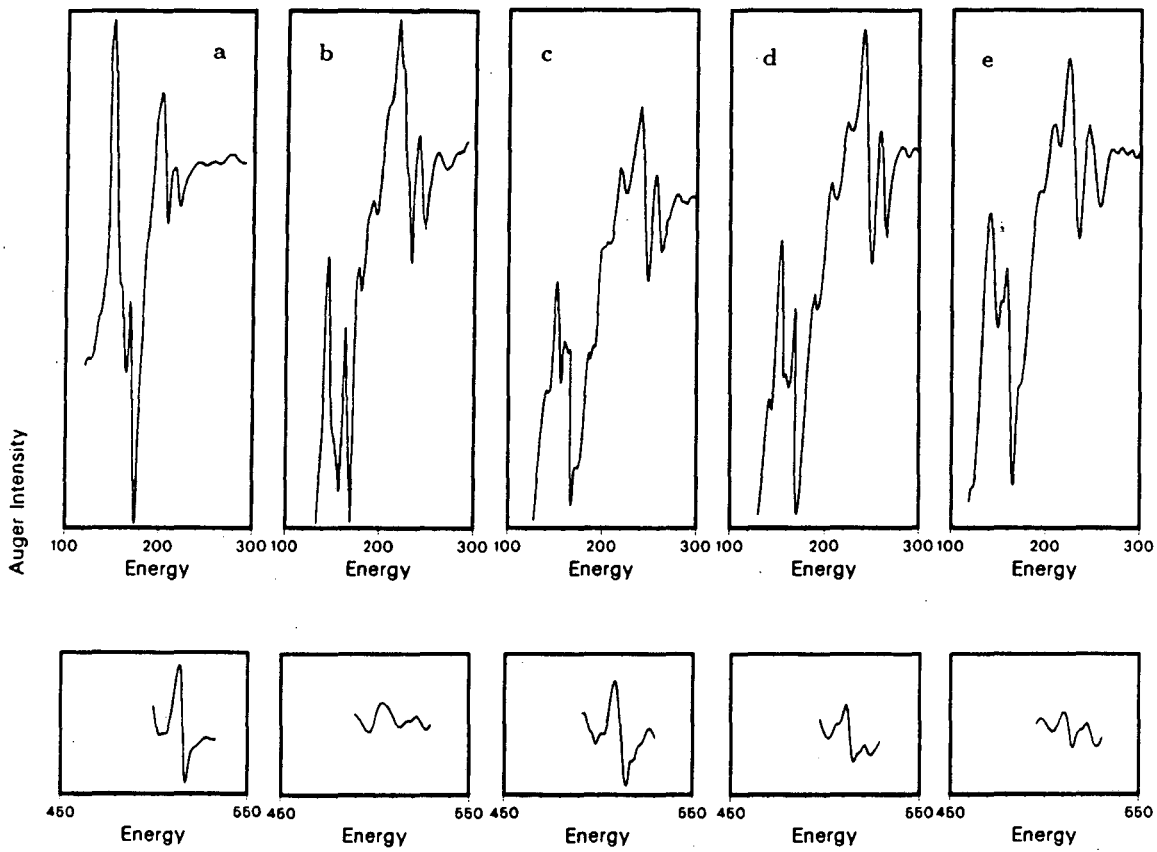

XBL 8711-4580

Fig. 6

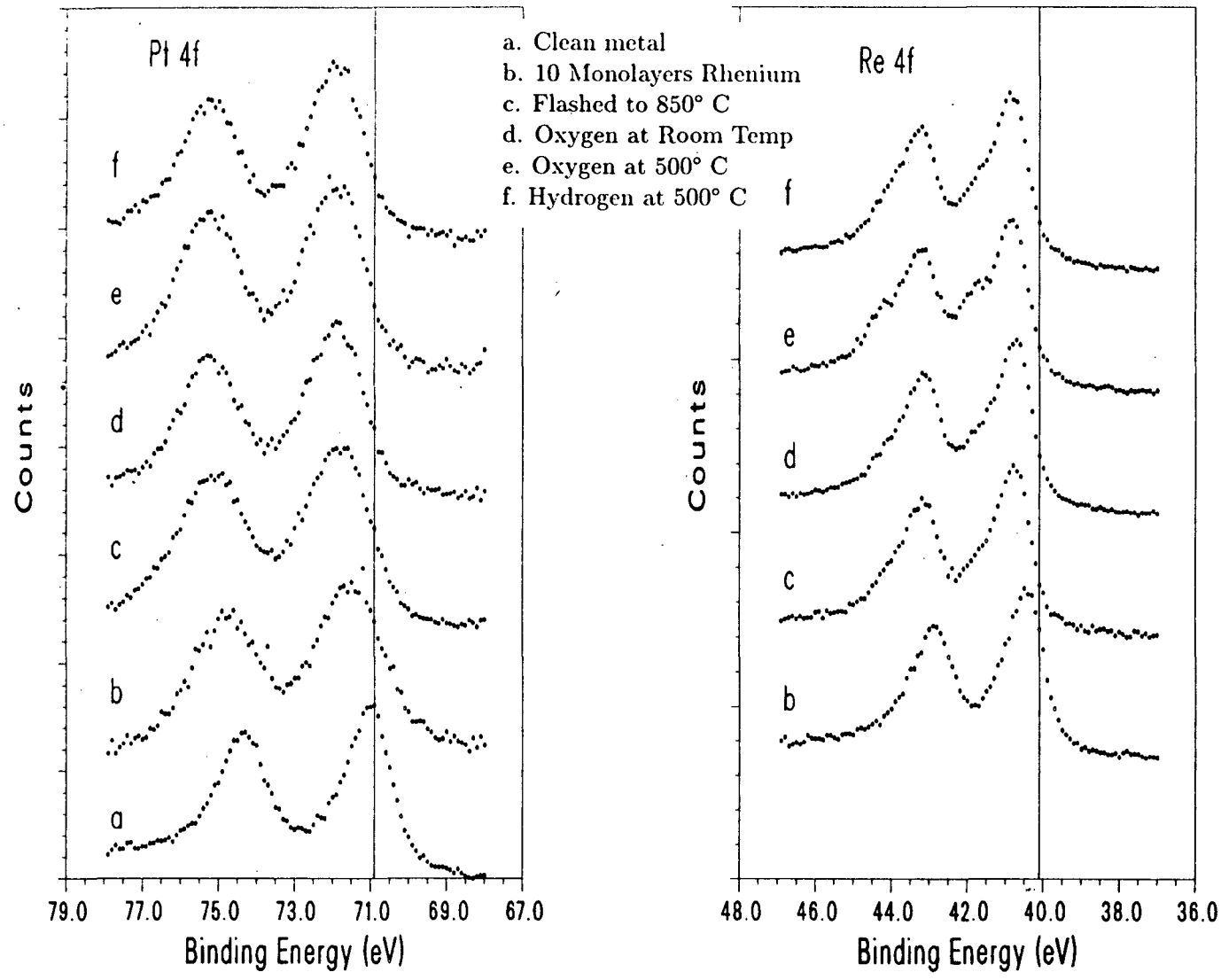

XBL 8711-4581

Fig. 7

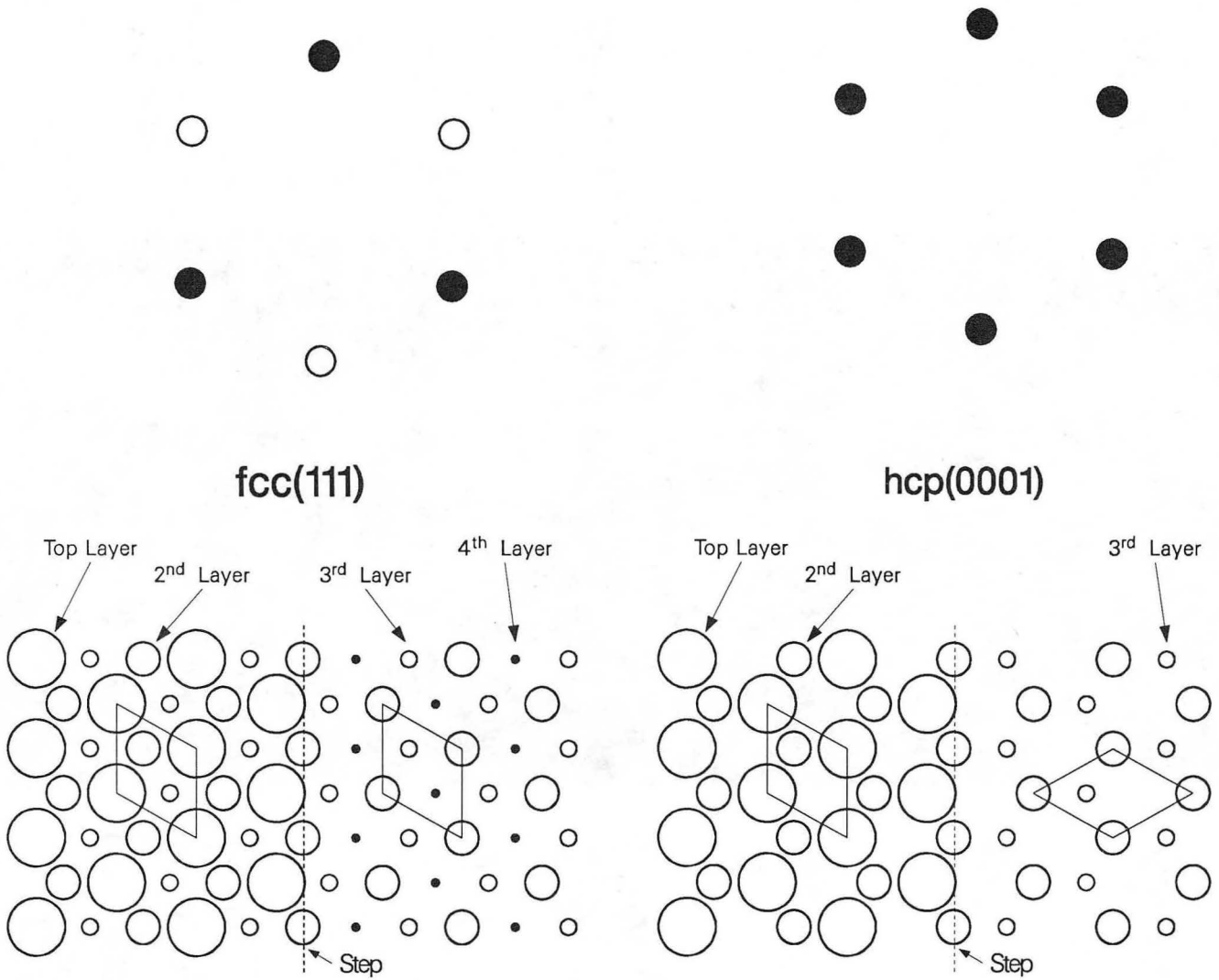

XBL 8711-4582

Fig. 8

Clean Pt(100)

70 eV

Pt(100) with 0.1 ML CO

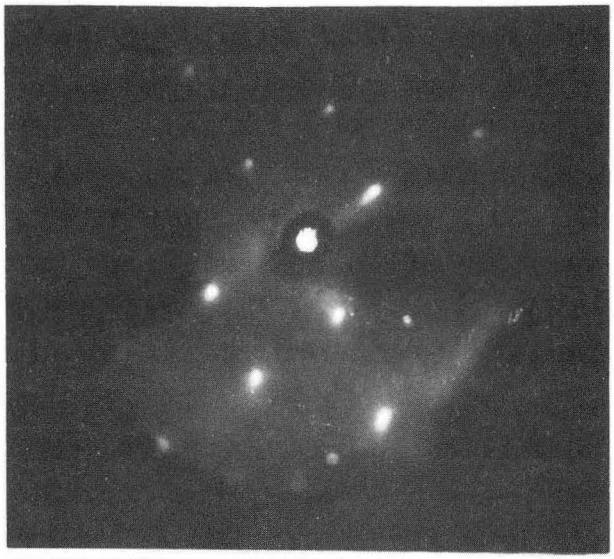

175 eV

Pt(100) with 15 ML Re Annealed to 800° C

195 eV

Fig. 9

LAWRENCE BERKELEY LABORATORY
TECHNICAL INFORMATION DEPARTMENT
UNIVERSITY OF CALIFORNIA
BERKELEY, CALIFORNIA 94720